1,4,5,6,7,8-Hexahydropyrido[4,3-d]pyrimidine inhibits HepG2 cell proliferation, migration and invasion, and induces apoptosis through the upregulation of miR-26b-5p by targeting CDK8

HANLIN LUO, YANG YANG, YANQIU ZHOU, XIANYONG BAI and YUN HOU

Department of Histology and Embryology, College of Basic Medicine, Binzhou Medical University, Yantai, Shandong 264003, P.R. China

Received November 8, 2022; Accepted March 28, 2023

DOI: 10.3892/ol.2023.13846

Abstract. 1,4,5,6,7,8-Hexahydropyrido[4,3-d]pyrimidine (PPM) promotes apoptosis of HepG2 cells and serves a role in tumor suppression. However, the role of microRNA (miRNA) regulation in initiating apoptosis remains unclear. Therefore, the present study performed reverse transcription-quantitative PCR to investigate the association between PPM and miRNA, which demonstrated that PPM upregulated the expression of miR-26b-5p. Wound healing and Transwell assays showed that PPM inhibited the migration and invasion of HepG2 cells, and EdU staining experiments showed that PPM inhibited the proliferation of HepG2 cells. Transfection with miR-26b-5p inhibitor reversed the effects of PPM on HepG2 cells. Flow cytometry results showed that PPM promoted apoptosis of HepG2 cells by upregulating miRNA (miR)-26b-5p, and Western blotting results showed that PPM promoted the expression of apoptosis-associated protein Bax and inhibited the expression of Bcl-2 by upregulating miR-26b-5p. Using a proteomic approach combined with bioinformatics analysis, CDK8 was identified as a potential target of miR-26b-5p and was downregulated by miR-26b-5p overexpression. However, PPM induced HepG2 cell cycle arrest without the involvement of miR-26b-5p. Western blotting results showed that PPM upregulation of miR-26b-5p suppresses NF-κB/p65 signaling pathway in HepG2 cells by targeting of CDK8. The present results suggested that miR-26b-5p may function as a target gene of PPM and may serve a role in hepatocellular carcinoma treatment.

Correspondence to: Professor Yun Hou or Professor Xianyong Bai, Department of Histology and Embryology, College of Basic Medicine, Binzhou Medical University, 346 Guanhai Road, Laishan, Yantai, Shandong 264003, P.R. China
E-mail: houyun820424@163.com
E-mail: xybai1963@126.com

Key words: 1,4,5,6,7,8-hexahydropyrido[4,3-d]pyrimidine, microRNA-26b-5p, apoptosis, CDK8, cell invasion

Introduction

Hepatocellular carcinoma (HCC) is the most common form of liver cancer, which accounts for ~80% of liver cancer cases; the number of cases in China exceeds 400,000 per year (1). Liver cancer is difficult to diagnose in its early stages and, thus, has a poor prognosis in the later stages; patients with liver cancer have a poor prognosis and a low five-year survival rate (1,2). Therefore, it is important to identify effective therapeutic drugs (2). Curcumin is extracted from the rhizome of turmeric, zedoary and other ginger plants; it has a variety of pharmacological activities, including anti-inflammatory, antioxidant, lipid-lowering and anti-tumor effects (3). However, its low stability and poor bioavailability limit its clinical application (3). To improve its anti-tumor effects and bioavailability, structural modification and optimization of curcumin are performed. For example, transformation of a central double α,β-unsaturated ketone into a piperidone-related α,β-unsaturated ketone to yield (3E,5E)-3,5-bis(arylidene)-4-piperidone (BAP) derivatives (4,5). Symmetrical and unsymmetrical BAPs with a variety of substituents on both sides, such as pyridine-, methoxy-, halogen- and nitro-, have been proven to have both antitumor and anti-inflammatory activity by inhibiting the activation of NF-κB and MAPK signal pathways (6). However, BAPs still have the disadvantages of having low water solubility and high toxicity (6). For optimization of physicochemical properties of BAPs, novel 1,4,5,6,7,8-hexahydropyrido[4,3-d]pyrimidine (PPM) derivatives based on scaffold hopping have been generated through Michael condensation reaction between BAPs and guanidine hydrochloride; PPMs are obtained from the structural optimization of curcumin and BAPs (7,8). Recently, certain fluoro- or trifluoromethyl-substituted PPMs have been reported to exhibit increased water solubility and decreased toxicity of human wild-type (wt) hepatocytes, but increased cytotoxicity to the liver cancer cells compared with curcumin and BAPs (7,8). More importantly, PPM serves a potential anti-hepatoma role by increasing Bax and Caspase-3 expression and decreasing Bcl-2 expression, as well as inducing HepG2 cell apoptosis by inhibiting the activation of NF-κB signaling (8). The present study aimed to investigate the underlying mechanisms to understand the role of PPM in preventing HCC.

MicroRNAs (miRNAs) regulate biological functions, serve as a diagnostic tool for cancer and are involved in tumorigenesis and cancer progression by pairing with the 3'-untranslated region (UTR) of mRNA to increase or decrease mRNA translation (9-11). miRNA (miR)-26-5p increased the sensitivity of breast cancer cells toward chemotherapeutic drugs and inhibited the migration and invasion of tumor cells (12). In bladder cancer cells, miR-26a/b-5p regulates migration and invasion (13). miR-26b-5p inhibits HCC cells migration and invasion (14). Both miR-26b-5p and heat shock 70 kDa protein 8 are molecular targets for selectively eliminating epithelial cancer stem cells in human HCC (14,15). miR-26b-5p is involved in the induction of apoptosis in ovarian granulosa cells of rats, whereas downregulation of miR-26b-5p inhibits Bax and promotes the expression of Bcl-2, thereby inhibiting apoptosis (16). In A549 lung adenocarcinoma cells, miR-26b-5p mimics inhibit expression of Bcl-2 and induce apoptosis (17). miR-26b-5p can promote the apoptosis of SKOV3 ovarian cancer cells by regulating the expression of Bax and Bcl-2 (18). miR-26b can promote the expression of Bax and Caspase 3, and increase apoptosis of liver cancer cells (19). In addition, miR-26b-5p may regulate NF-κB activation; miR-26b inhibits the expression of IκB and phosphorylated (p-)p65 by targeting the proteins TGF-β-activated kinase 1 and TGF-β-activated kinase 1/MAP3K7 binding protein 3, thus inhibiting NF-κB signaling and increasing sensitivity of liver cancer cells to apoptosis (20). miR-26b was also reported to inhibit PI3K/AKT/NF-κB signaling (19).

The present study aimed to investigate the biological roles of PPM in HepG2 cells, its effects on miR-26b-5p expression and whether PPM has an anti-liver cancer role by regulating miR-26b-5p. Proliferation, invasion and apoptosis assays, as well as western blotting and reverse transcription-quantitative PCR (RT-qPCR), were performed. Results from the present study identified some potential treatment methods and elucidated the mechanism by which PPM induces apoptosis in HCC cells. In addition, these results identified potential effective treatment mechanisms for HCC through miRNA-targeting treatments.

Materials and methods

Cell culture. The human hepatoma cancer cell line HepG2 was purchased from Nanjing KeyGen Biotech Co., Ltd. (cat. no. KG020). Short tandem repeat analysis showed that there was no cross contamination of human cells was found in the cell line. DNA typing of this cell line had 100% match with HepG2 cells obtained from American Type Culture Collection cell bank. Cells were cultured in HyClone DMEM with high glucose medium (Cytiva) containing 1% penicillin/streptomycin and 10% FBS (Newzerum, Ltd.) in humidified conditions with 5% CO_2 at 37˚C.

Cell transfection and PPM treatment. miR-26b-5p inhibitor, inhibitor negative control (NC), miR-26b-5p mimics and NC mimics were purchased from Shanghai GenePharma Co., Ltd. To investigate the effect of PPM on the expression of miR-26b-5p in HepG2 cells, cells were seeded ($1.5x10^5$ cells/well) and cultured at 37˚C for 24 h. Then, 2 μM PPM was added and the cells were incubated at 37˚C for an additional 24 h. miR-26b-5p inhibitor concentrations of 20, 50 and 80 nM were used to screen for the miR inhibitor concentration with the highest transfection efficiency; miR-26b-5p mimics and NC mimics were used at 50 nM. In the Inhibitor NC + PPM and Inhibitor + PPM group, HepG2 ($1.5x10^5$ cells/well) cells were seeded in 6-well plates, and transfection reagent Lipofectamine™ 2000 (Invitrogen; Thermo Fisher Scientific, Inc.) was added when cell density reached 30%, according to the manufacturer's instructions. Cells were transfected in serum-free HyClone DMEM with high glucose medium at 37˚C for 6 h. Following transfection, the medium was replaced with complete medium containing 10% FBS (Newzerum, Ltd.) and the cells were incubated for a further 24 h. A total of 2 μM PPM was added and the cells were incubated at 37˚C for 24 h. The sequences were as follows: miR-26b-5p inhibitor, 5'-ACCUAUCCUGAAUUA CUUGAA-3'; miR-26b-5p mimics forward, 5'-UUCAAGUAA UUCAGGAUAGGU-3' and reverse, 5'-CUAUCCUGAAUU ACUUGAAUU-3'; miR inhibitor NC 5'-CAGUACUUUUGU GUAGUACAA-3'; and miR mimics NC forward, 5'-UUCUCC GAACGUGUCACGUTT-3' and reverse, 5'-ACGUGACAC GUUCGGAGAATT-3'. Transfection efficiency was determined using RT-qPCR.

RNA extraction and RT-qPCR analysis. To detect the effect of PPM on miR-26b-5p expression, the experiment was divided into two groups: Untreated Control and PPM treatment. To screen the concentration of inhibitors, the experiment was divided into five groups: Control, Inhibitor NC, Inhibitor (20 nM), Inhibitor (50 nM), Inhibitor (80 nM). To detect the effect of inhibitors on miR-26b-5p expression after PPM addition, the experiment was divided into two groups: Inhibitor NC + PPM and Inhibitor + PPM. RNA was isolated from the different groups using TRIzol® reagent (Invitrogen; Thermo Fisher Scientific, Inc.), according to the manufacturer's instructions. RT-qPCR was used to measure the expression of miR-26b-5p. Total RNA was extracted from HepG2 cells using TRIzol reagent (Invitrogen; Thermo Fisher Scientific, Inc.). The RNA was reverse-transcribed into cDNA using the SPARKscript II RT Plus kit with gDNA Eraser (cat. no. AG0304; Shandong Sparkjade Scientific Instruments Co., Ltd.), according to the manufacturer's protocol, and amplification was performed using a 2X SYBR Green qPCR Mix (with ROX) kit (cat. no. AH0104; Shandong Sparkjade Scientific Instruments Co., Ltd.). Using 0.2 μl cDNA as the template, thermocycling was performed as follows: 94˚C for 3 min; followed by 40 cycles of 94˚C for 15 sec, 60˚C for 15 sec and 72˚C for 25 sec. β-actin was used as a housekeeping gene. β-actin and miR-26b-5p primers were designed and synthesized by Shanghai Shenggong Biology Engineering Technology Service, Ltd. Changes in miR-26b-5p expression levels were calculated using the $2^{-\Delta\Delta Cq}$ method (18). The primer sequences were as follows: miR-26b-5p forward, 5'-CCGGGA CCCAGTTCAAGTAA-3' and reverse, 5'-CCCCGAGCCAAG TAATGGAG-3' and β-actin forward, 5'-TGGCACCCAGCA CAATGAA-3' and reverse, 5'-CTAAGTCATAGTCCGCCT AGAAGCA-3'.

Wound healing assay. HepG2 cells were transfected with miR-26b-5p or inhibitor NC for 24 h at 37˚C when the cell density reached 30%, followed by treatment with PPM for 24 h

at 37˚C. When the cells reached 90% confluence, a scratch was made with a 200 μl pipette tip and debris was washed with PBS; the cells were then cultured in serum-free medium at 37˚C. At 0 and 48 h, the wound was observed with an inverted light microscope (Olympus Corporation) at x100 magnification, and images were captured for analysis.

Transwell migration and invasion assay. The migratory and invasive abilities of HepG2 cells were examined using Transwell chambers with 8 μm pore membranes (Guangzhou Jet Bio-Filtration Co., Ltd.). Following miR-26b-5p inhibitor transfection and PPM treatment, HepG2 cells were seeded ($2.5x10^4$ cells/well) into the upper chamber containing HyClone DMEM with high glucose medium (Cytiva). The lower chamber was filled with complete medium containing 10% FBS (Newzerum, Ltd.), After 24 h of incubation at 37˚C, cells in the upper chamber were removed and those migrating into the lower chamber were fixed with 4% paraformaldehyde for 15 min and stained with 0.1% crystal violet (Beyotime Institute of Biotechnology) for 10 min, both at room temperature. A total of five randomly selected fields of view were captured under a light microscope (Zeiss AG) at x200 magnification. ImageJ v1.53a (National Institutes of Health,) was used to count the migrated cells.

For the cell invasion assay, the upper chamber was precoated with Matrigel (dilution, 1:9; Corning Inc.) at 4˚C for 12 h. HepG2 cells were seeded ($2.5x10^4$ cells/well) in tissue culture plate inserts coated with Matrigel (Corning Inc.) at 37˚C for 6 h. The subsequent procedures were the same as for the cell migration assay.

EdU proliferation assay. For the cell proliferation assay, HepG2 cells were seeded ($2.5x10^4$ cells/well) into 24-well plates at 37˚C for 24 h. Subsequently, cells were transfected with miR-26b-5p inhibitor for 24 h, then treated with 2 μM PPM for 37˚C for 24 h. Cell proliferation was detected using BeyoClick™ EdU-488 Cell Proliferation Assay kit (Beyotime Institute of Biotechnology) according to the manufacturer's protocol. Briefly, the cells were incubated with EdU solution for 2 h at 37˚C, fixed with 4% paraformaldehyde for 15 min and then washed with PBS three times, both at room temperature. To perforate the cells, PBS containing 0.3% Triton X-100 was added for 10 min at 37˚C, and the Click Additive solution (provided in the kit) was added and the cells were incubated at room temperature for 30 min in the dark. Nuclei were stained with 100 μl Hoechst (1,000X diluted to 1:1,000) in dark for 10 min at 37˚C. After washing with PBS, cells were observed under a fluorescence microscope (Echo) at x100 magnification, and images were analyzed using ImageJ v1.53a (National Institutes of Health).

Western blotting. HepG2 cells were lysed using RIPA lysis buffer (Beyotime Institute of Biotechnology) and collected by centrifugation (16,904 x g for 15 min at 4˚C) to extract the total protein. BCA protein concentration kit (Beyotime Institute of Biotechnology) was used to quantify protein concentration. A total of 20 μg protein/lane was separated by 10% SDS-PAGE and transferred onto PVDF membranes for 1.5 h at 200 mA. Following blocking with 5% skimmed milk for 1 h at room temperature, the membranes were incubated overnight at 4˚C with the following rabbit primary antibodies: Rabbit polyclonal anti-Bax (1:2,000; cat. no. 50599-2-Ig) and anti-GAPDH (1:10,000; cat. no. 10494-1-AP) from Proteintech Group, Inc.; monoclonal anti-Bcl-2 (1:2,000; cat. no. A19693) from ABclonal Technology; anti-p65 (cat. no. 4767) and anti-p-p65 (both 1:2,000; cat. no. 3033S) from Cell Signaling Technology, Inc.; and anti-CDK8 (1:2,000; cat. no. AF2467) from Beyotime Institute of Biotechnology. The PVDF membranes were then incubated with an HRP-conjugated goat anti-rabbit IgG H&L antibody (1:5,000; cat. no. SA00001-2; Proteintech Group, Inc.) for 1 h at room temperature. The membranes were washed with TBST containing 1% Tween 20 (BioFroxx; NeoFroxx GmbH) and Super Excellent Chemiluminescent Substrate (ECL) Detection kit reagent (cat. no. E-IR-R308; Elabscience, Co., Ltd.) was added dropwise onto the PVDF membrane. The immunoreactive bands were detected using a Tanon 4600SF chemiluminescence imaging system (Tanon Science and Technology Co., Ltd.), and the relative levels of each protein were semi-quantified using ImageJ v1.53a (National Institutes of Health).

Apoptosis assay. The Annexin V-FITC Cell Apoptosis kit (cat. no. G003-1; Nanjing Jiancheng Bioengineering Institute) was used to determine apoptotic rates according to the manufacturer's instructions. HepG2 cells were seeded ($1.5x10^5$ cells/well) in 6-well plates and transfected with inhibitor NC, miR-26b-5p inhibitor, inhibitor NC + PPM or inhibitor + PPM for 24 h, then 2 μM PPM was added and the cells were incubated at 37˚C for 24 h. Cells were washed with cold PBS and pelleted by centrifugation at 1,000 x g for 5 min at room temperature. Then, the cells were resuspended in 1X Annexin-binding buffer (500 μl) and 5 μl each Annexin V-FITC and PI was added to the binding solution and mixed according to the manufacturer's instructions. After 10 min at room temperature, cell apoptosis was analyzed using FACSCanto™ II flow cytometer (BD Biosciences). Total apoptosis included early and late apoptotic cells, and the results were analyzed using FACSDiva Version 6.1.3 (BD Biosciences).

Cell cycle assay. For the cell cycle assay, a PI Cell Cycle and Apoptosis kit (cat. no. abs50005; Absin Bioscience, Inc.) was used. HepG2 cells were seeded ($1.5x10^5$ cells/well) in 6-well plates at 37˚C for 24 h. When the cells reached 30% confluence, they were transfected with miR-26b inhibitor or inhibitor NC for 24 h, with or without subsequent treatment with 2 μM PPM for 37˚C for 24 h. Cells were collected by centrifugation at 1,000 x g for 5 min at room temperature. A total of 1 ml 70% ethanol was added to each well and incubated at 4˚C for 18 h for fixation. Cells were then washed with PBS and centrifuged at 1,000 x g for 5 min at room temperature. The cell pellets were resuspended in 100 μl propidium iodide staining buffer and stained with PI working solution for 30 min at room temperature in the dark. The cells were analyzed by FACSCanto™ II flow cytometry (BD Biosciences), and ModFit LT V4.1.7 software (Verity Software House) was used to analyze the DNA content.

Bioinformatics. TargetScan (www.targetscan.org/vert_72), miRDB (www.mirdb.org) and Starbase (https://starbase.sysu.edu.cn/starbase2) were used to predict downstream targets of

miR-26b-5p, as well as the binding site between miR-26b-5p and the target mRNAs.

NCBI (http://www.ncbi.nlm.nih.gov) was used to find the 3'-UTR of the target mRNA as well as to design the plasmid vector according to the binding site between miR-26b-5p and the target mRNA, which was experimentally validated by dual-luciferase reporter gene assay.

Dual-luciferase reporter gene assay. miR-26b-5p mimics, NC mimics and the Dual Luciferase Reporter Assay kit were purchased from Shanghai GenePharma Co., Ltd. wt and mutant (mut) plasmids of CDK8 (pmirGLO-CDK8-wt and pmirGLO-CDK8-mut) were designed by Shandong Scientific Cloud Biotechnology Co., Ltd. Both wt and mut 3'-UTRs of CDK8 mRNAs were cloned and inserted downstream of firefly luciferase in the pmiRGLO vector. HepG2 cells were seeded ($1.5x10^5$ cells/well) in 6-well plates. When the cell density reached 30%, they were co-transfected, using 8 μl Lipofectamine 2000, with either 1 μg wt or mut plasmid and 50 nM of either miR-26b-5p mimics or mimics NC, transfected; after 6 h, the cells were incubated in complete medium containing 10% FBS (Newzerum, Ltd.) for 24 h at 37˚C. Cells were collected and luciferase activities were detected using the Dual Luciferase Reporter Assay, according to the manufacturer's instructions. Firefly luciferase activity was normalized to *Renilla* luciferase activity.

Construction of CDK8 overexpression vector. The human CDK8 coding sequences (NM_001346501) were obtained from NCBI (http://www.ncbi.nlm.nih.gov). CDK8 overexpression plasmid of HepG2 cells were purchased from KeyBio Scientific, Inc. The HepG2 cells were seeded, at a density of $1.5x10^5$ cells/well in six-well plates and incubated for at 37˚C 24 h. HepG2 cells grown to 30% confluence were transfected with 8 μl Lipofectamine 2000 and 1 μg plasmid, Cells were incubated at 37˚C for 2 days, followed by extraction of cellular proteins.

Statistical analysis. Data are expressed as the mean ± SD; experiments were repeated in triplicate. Comparisons between groups were performed using one-way analysis of variance using GraphPad Prism v8.0.1 (Dotmatics) followed by Bonferroni's correction. $P<0.05$ was considered to indicate a statistically significant difference.

Results

PPM upregulates expression of miR-26b-5p in HepG2 cells. RT-qPCR was performed to determine the effects of PPM treatment on the expression of miR-26b-5p. PPM significantly increased the expression of miR-26b-5p compared with the Control group (untreated cells) (Fig. 1A). To investigate the effects of miR-26b-5p inhibition, cells were transfected with varying concentrations of miR-26b-5p. miR-26b-5p inhibitor transfection at 50 nM induced the greatest inhibition of miR-26b-5p expression compared with the Control group. The knockdown efficiency of the inhibitor at 80 nM was lower compared with that of 50 nM, likely because high concentration of Inhibitor may lead to the increased of off-target effects and cytotoxicity to cells, thereby reducing the transfection efficiency. Therefore, 50 nM was selected for subsequent experiments (Fig. 1B). RT-qPCR was used to determine the relative expression levels of miR-26b-5p in liver cancer cells. The results demonstrated that miR-26b-5p expression levels were downregulated in Inhibitor + PPM group compared with Inhibitor NC + PPM group (Fig. 1C).

PPM inhibits migration of HepG2 cells by upregulating miR-26b-5p. Wound healing and Transwell assays were performed to examine cell migration. Wound closure increased in the Inhibitor group and decreased in the PPM group compared with the untreated Control group (Fig. 2A and B). Cells transfected with miR-26b-5p inhibitor alleviated the PPM-induced inhibition of HepG2 cell migration. The number of migrating cells increased in the miR-26b-5p Inhibitor group, but decreased in the PPM-treated group compared with Inhibitor + PPM group (Fig. 2C and D). These results suggested that PPM may inhibit HepG2 cell migration by upregulating miR-26b-5p.

PPM inhibits the invasion of HepG2 cells by upregulating miR-26b-5p. Transwell invasion assay results showed that PPM significantly decreased the cell invasion rate, whereas miR-26b-5p inhibitor transfection significantly increased cell invasion, as compared with the Control group (Fig. 2E and F). PPM significantly inhibited the invasion of HepG2 cells, as compared with Inhibitor + PPM group. These results indicated that PPM inhibited the invasion of HepG2 cells by upregulating miR-26b-5p.

PPM inhibits HepG2 cell proliferation by upregulating miR-26b-5p. EdU staining was performed to determine whether PPM inhibited the proliferation of HepG2 cells through miR-26b-5p. PPM treatment significantly decreased the number of EdU-positive cells compared with the Control group (Fig. 3), whereas miR-26b-5p inhibitor alone significantly increased the EdU-positive cells. PPM significantly decreased proliferation of HepG2 cells compared with Inhibitor + PPM group. These results suggested that PPM may inhibit the proliferation of HepG2 cells by upregulating miR-26b-5p.

PPM promotes HepG2 cell apoptosis by upregulating miR-26b-5p. An Annexin V-FITC/PI staining kit was used to investigate the effects of PPM treatment on apoptosis by upregulating miR-26b-5p. In the Control, Inhibitor NC and Inhibitor group, the mean apoptotic rate of HepG2 cells was 5.5, 7.1 and 2.5%, respectively, demonstrating that miR-26b-5p inhibition decreased apoptosis compared with the Control group (Fig. 4A and B). When treated with PPM, the mean apoptotic rates in these groups increased to 11.3, 11.5 and 5.4%, respectively, indicating that PPM significantly increased apoptosis, and that miR-26b-5p Inhibitor group significantly decreased the apoptosis compared with Inhibitor + PPM group. These results suggested that PPM may promote apoptosis by upregulating miR-26b-5p.

Results from western blotting demonstrated that PPM treatment significantly increased Bax and decreased Bcl-2 compared with the Control group. The miR-26b-5p Inhibitor significantly decreased Bax but increased Bcl-2 compared with

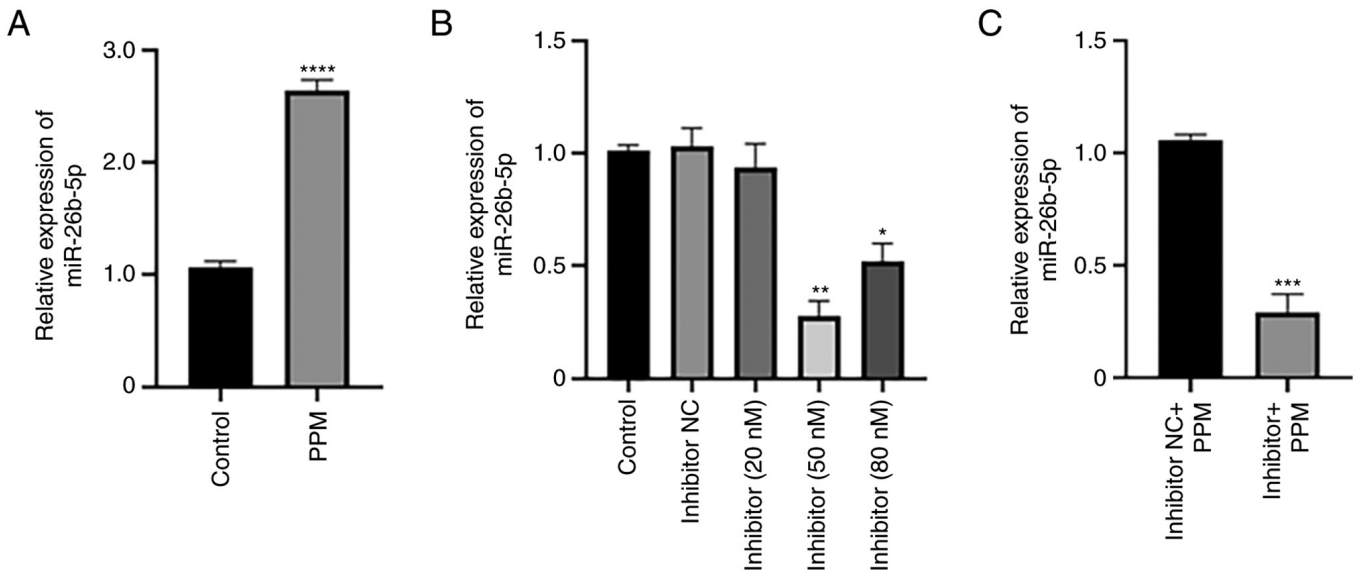

Figure 1. PPM upregulates expression of miR-26b-5p. Reverse transcription-quantitative PCR analysis of miR-26b-5p expression in HepG2 cells following treatment with (A) PPM and (B) miR-26b-5p inhibitor at various concentrations. (C) The effect of miR-26b-5p inhibitor and PPM on miR-26b-5p expression. Data are presented as the mean ± SD. *P<0.05, **P<0.01, ***P<0.001 and *****P<0.0001 vs. Control. miR, microRNA; NC, negative control; PPM, 1,4,5,6,7,8-hexahydropyrido[4,3-d]pyrimidine.

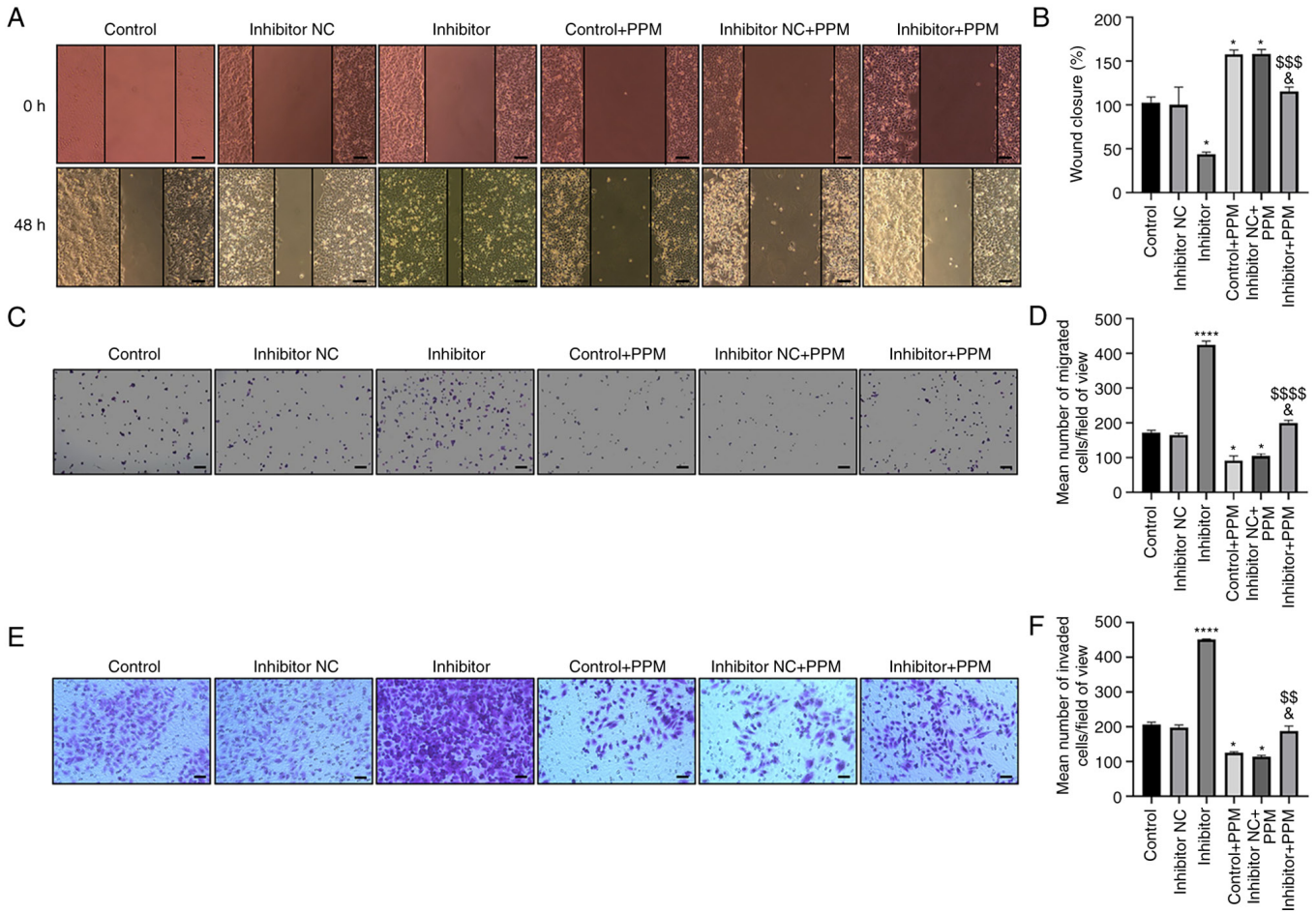

Figure 2. PPM inhibits migration and invasion of HepG2 cells through upregulation of miR-26b-5p. (A) Wound healing assay was used to detect the effect of PPM upregulation of miR-26b-5p on migration of HepG2 cells. Scale bar, 100 μm. (B) Quantitated wound healing area from part (A). (C) Transwell assays were used to detect the effect of PPM on cell migration. Scale bar, 200 μm. (D) Average number of migrated cells from part (C). (E) Transwell Matrigel assays were used to detect the effect of PPM on cell invasion. Scale bar, 50 μm. (F) Average number of invaded cells from part (E). *P<0.05, ****P<0.0001 vs. Control; $^{\&}$P<0.05 vs. Control + PPM; $^{\$\$}$P<0.01, $^{\$\$\$}$P<0.001, $^{\$\$\$\$}$P<0.0001 vs. Inhibitor. miR, microRNA; NC, negative control; PPM, 1,4,5,6,7,8-hexahydropyrido[4,3-d] pyrimidine.

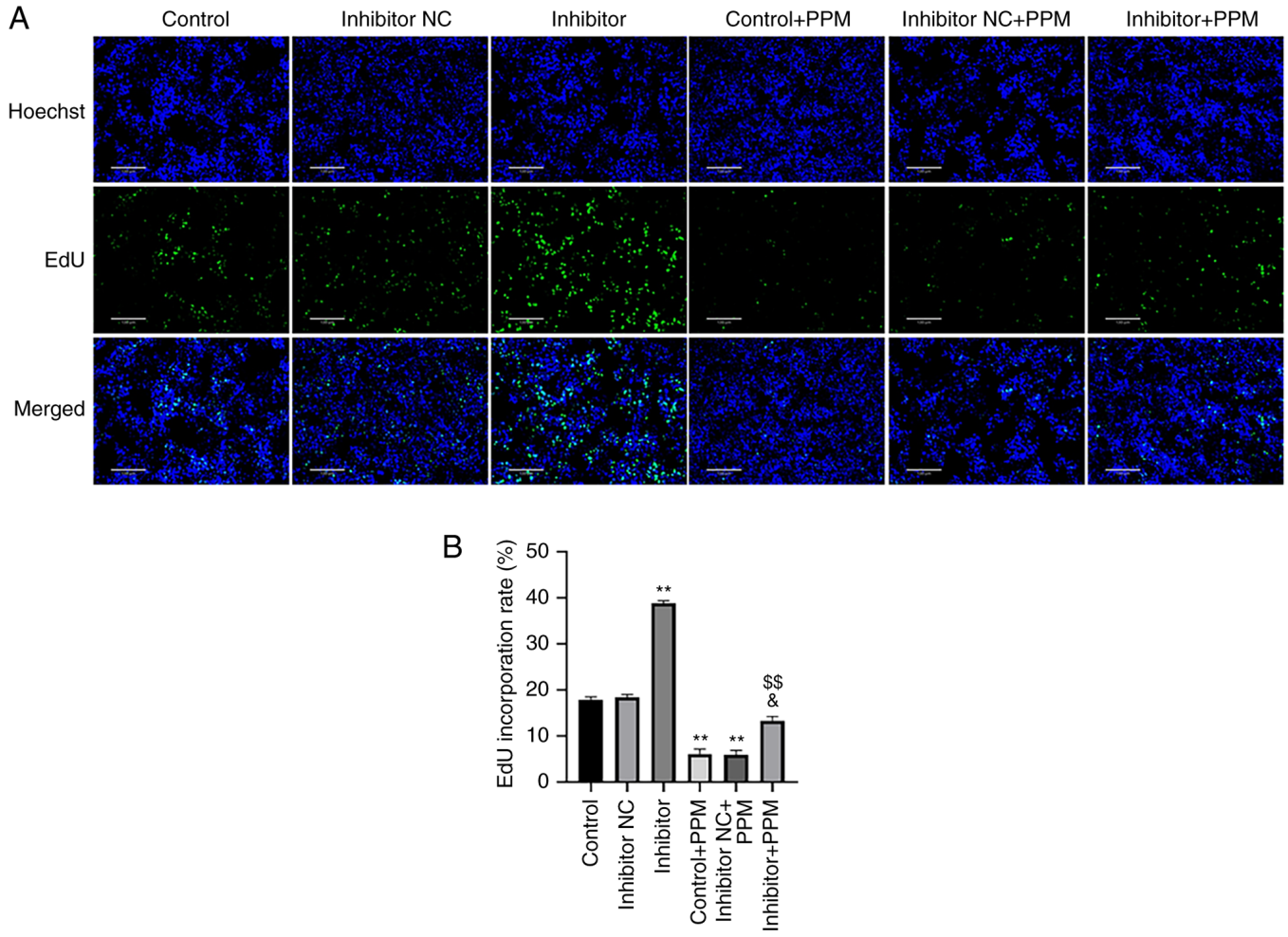

Figure 3. PPM inhibits proliferation of HepG2 cells through upregulation of miR-26b-5p. (A) EdU staining was used to detect proliferating HepG2 cells. Scale bar, 130 μm. (B) Percentage of EdU-positive cells. **P<0.01 vs. Control; $^{\&}$P<0.05 vs. Control + PPM; $^{\$\$}$P<0.01 vs. Inhibitor. NC, negative control; PPM, 1,4,5,6,7,8-hexahydropyrido[4,3-d]pyrimidine.

the Control group. However, PPM co-treatment significantly inhibited the miR-26b-5p inhibitor-induced increased expression of Bax and decreased expression of Bcl-2 (Fig. 4C-E). miR-26b-5p inhibitor significantly reduced the expression ratio of Bax/Bcl-2 compared with the Control, whereas PPM significantly increased expression ratio of Bax/Bcl-2, PPM co-treatment significantly reduced the expression ratio of Bax/Bcl-2 compared with the PPM group (Fig. 4F). These results suggested that PPM may promote the expression of Bax and reduced the expression of Bcl-2 by upregulating miR-26b-5p in HepG2 cells.

PPM arrests HepG2 cells in the G_0/G_1 phase without the involvement of miR-26b-5p. The percentage of cells in the G_0/G_1, S and G_2/M phases was analyzed using flow cytometry. The percentage of G_0/G_1 cells in the Control, miR-26b-5p Inhibitor NC and miR-26b-5p Inhibitor group was 22.44, 21.10 and 22.48%, respectively (Fig. 5A and B), indicating that miR-26b-5p inhibitor did not regulate the cell cycle in HepG2 cells. When treated with PPM, the percentage of G_0/G_1 cells was 40.92, 37.56 and 37.54%, in the Control, miR-26b-5p Inhibitor NC and miR-26b-5p Inhibitor groups, respectively (Fig. 5A and B), indicating that PPM significantly increased cell count in the G_0/G_1 phase. Collectively, these data indicated that PPM arrested HepG2 cell cycle in G_0/G_1 phase independently of miR-26b-5p.

CDK8 is a target gene of miR-26b-5p. To study the mechanism by which miR-26b-5p controls HepG2 proliferation, invasion and apoptosis, the target genes of miR-26b-5p were predicted using TargetScan, miRDB and Starbase, which identified 1,045, 1,134 and 2,018 miR-26b-5p target genes, respectively, with 494 overlapping genes (Fig. 6A). CDK8 was predicted to be the target gene of miR-26b-5p; a recent study reported the involvement of CDK8 in the progression of HepG2, and binding sites between miR-26b-5p and CDK8 were identified (14). The 3'-UTR of CDK8 mRNA has three predicted miR-26b-5p target sites; in the present study, the first target site was mutated (192-198 sequence) as inserted into a dual-luciferase reporter assay plasmid containing a part of the CDK8 3'-UTR was used (Fig. 6B). miR-26b-5p mimics transfection upregulated the expression of miR-26b-5p (Fig. 6C). The results of the dual-luciferase reporter assay demonstrated that miR-26b-5p significantly suppressed the relative luciferase activity of the pmirGLO-CDK8-wt compared with pmirGLO-CDK8-mut (Fig. 6D); however, no suppression

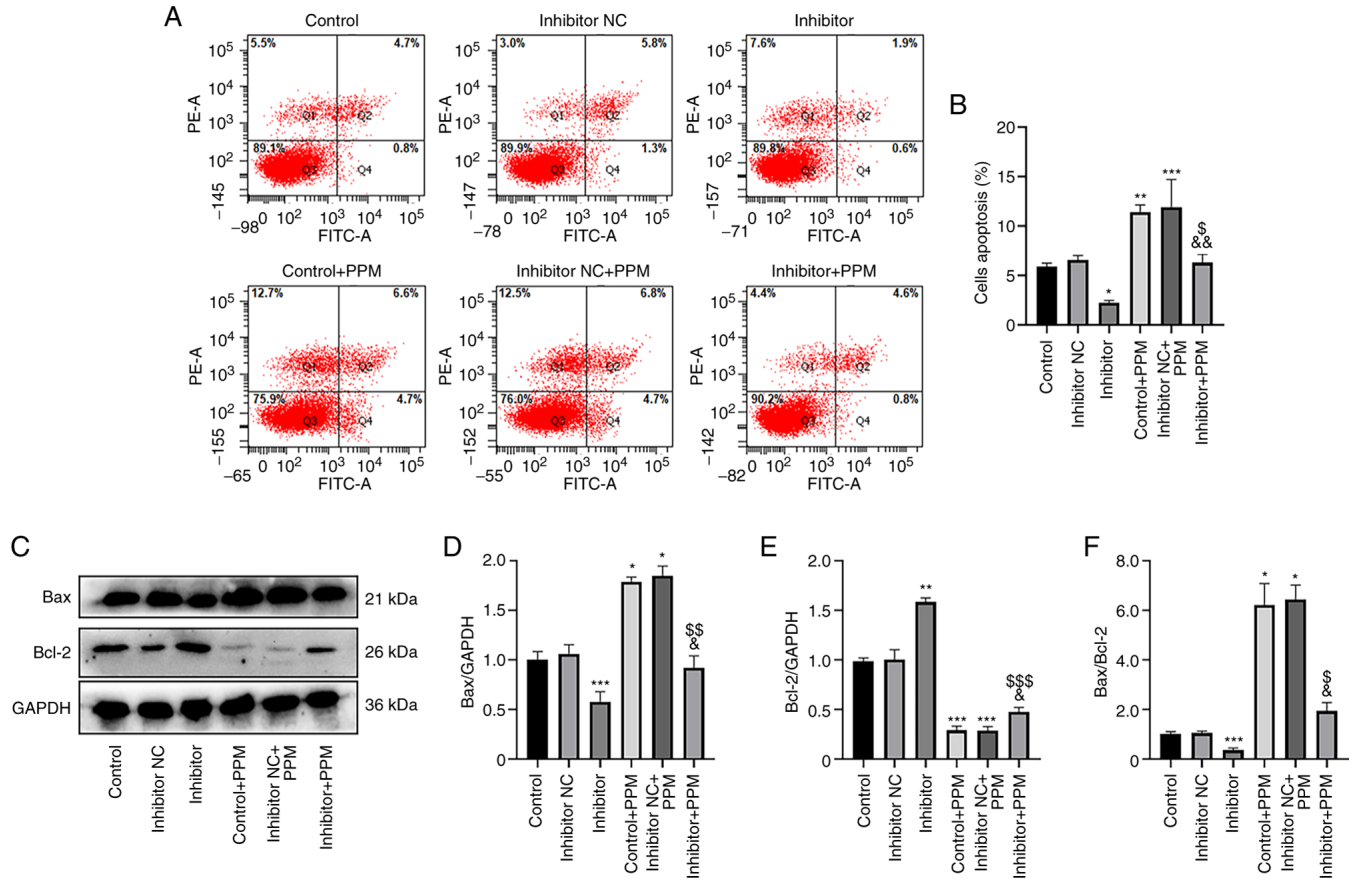

Figure 4. PPM promotes apoptosis and Bax/Bcl2 ratio through upregulation of miR-26b-5p in HepG2 cells. (A) Flow cytometry was used to analyze apoptosis in HepG2 cells. (B) Histograms presenting the percentage of apoptotic cells in the various groups. (C) The protein expression levels of Bax and Bcl-2 in HepG2 cells were detected by western blotting. Relative protein expression levels of (D) Bax and (E) Bcl-2; GAPDH was used as the internal control. (F) The Bax/Bcl-2 ratio in the different groups. *P<0.05, **P<0.01, ***P<0.001 vs. Control; $^{\&}$P<0.05, $^{\&\&}$P<0.01 vs. Control + PPM; $^{\$}$P<0.05, $^{\$\$}$P<0.01, $^{\$\$\$}$P<0.001 vs. Inhibitor. miR, microRNA; NC, negative control; PPM, 1,4,5,6,7,8-hexahydropyrido[4,3-d]pyrimidine.

in luciferase activity was observed with the mut 3'-UTR of CDK8. These results indicated the presence of binding sites between CDK8 and miR-26b-5p.

Western blot assay results demonstrated that miR-26b-5p negatively regulated CDK8 levels in HepG2 cells; that is, miR-26b-5p inhibitor transfection significantly increased the expression of CDK8 compared with the Control, whereas PPM significantly decreased CDK8 expression. PPM co-treatment significantly decreased the miR-26b-5p inhibitor-induced expression of CDK8 of HepG2 cells (Fig. 6E and F). Taken together, these results indicated that CDK8 is a target of miR-26b-5p.

PPM upregulation of miR-26b-5p suppresses NF-κB/p65 signaling pathway in HepG2 cells by targeting of CDK8. NF-κB activation is associated with apoptosis and tumorigenesis (12). PPM treatment inhibited phosphorylation of NF-κB/p65 compared with the Control group (Fig. 6G and H). PPM co-treatment significantly inhibited NF-κB/p65 activation induced by miR-26b-5p inhibitor (Fig. 6G and H). CDK8-OE vector transfection significantly increased the CDK8 expression compared with the CDK8-NC group (Fig. 6I and J). CDK8-OE promoted activation of NF-κB/p65, whereas PPM significantly inhibited NF-κB/p65 activation induced by CDK8-OE group (Fig. 6K and L). These results suggested that PPM upregulation of miR-26b-5p suppresses NF-κB/p65 signaling pathway in HepG2 cells by targeting of CDK8.

Discussion

PPM induces HepG2 cell apoptosis by inhibiting NF-κB/p65 activation (8); however, it is still unknown whether microRNAs are involved in this process. The present study demonstrated that PPM treatment increased expression of miR-26b-5p and inhibited cell migration, proliferation and NF-κB/p65 activation. PPM also promoted cell apoptosis by upregulating miR-26b-5p.

miR-26b-5p serves an important role in many diseases, such as promoting angiogenesis and endothelial cell proliferation after acute ischemia (21). In addition, it disrupts cancer progression and EMT, and promotes apoptosis of tumor cells. For example, miR-26b-5p was reported to inhibit non-small cell lung cancer progression, promote apoptosis and enhance radiosensitivity in lung adenocarcinoma cells (22,23). miRNA-26b-5p also targets transcriptional repressor GATA binding 1 mRNA to promote apoptosis of breast cancer cells and inhibit their proliferation (24). In addition, miR-26b-5p inhibits EMT, migration and invasion of HCC cells. It also promotes expression of apoptotic

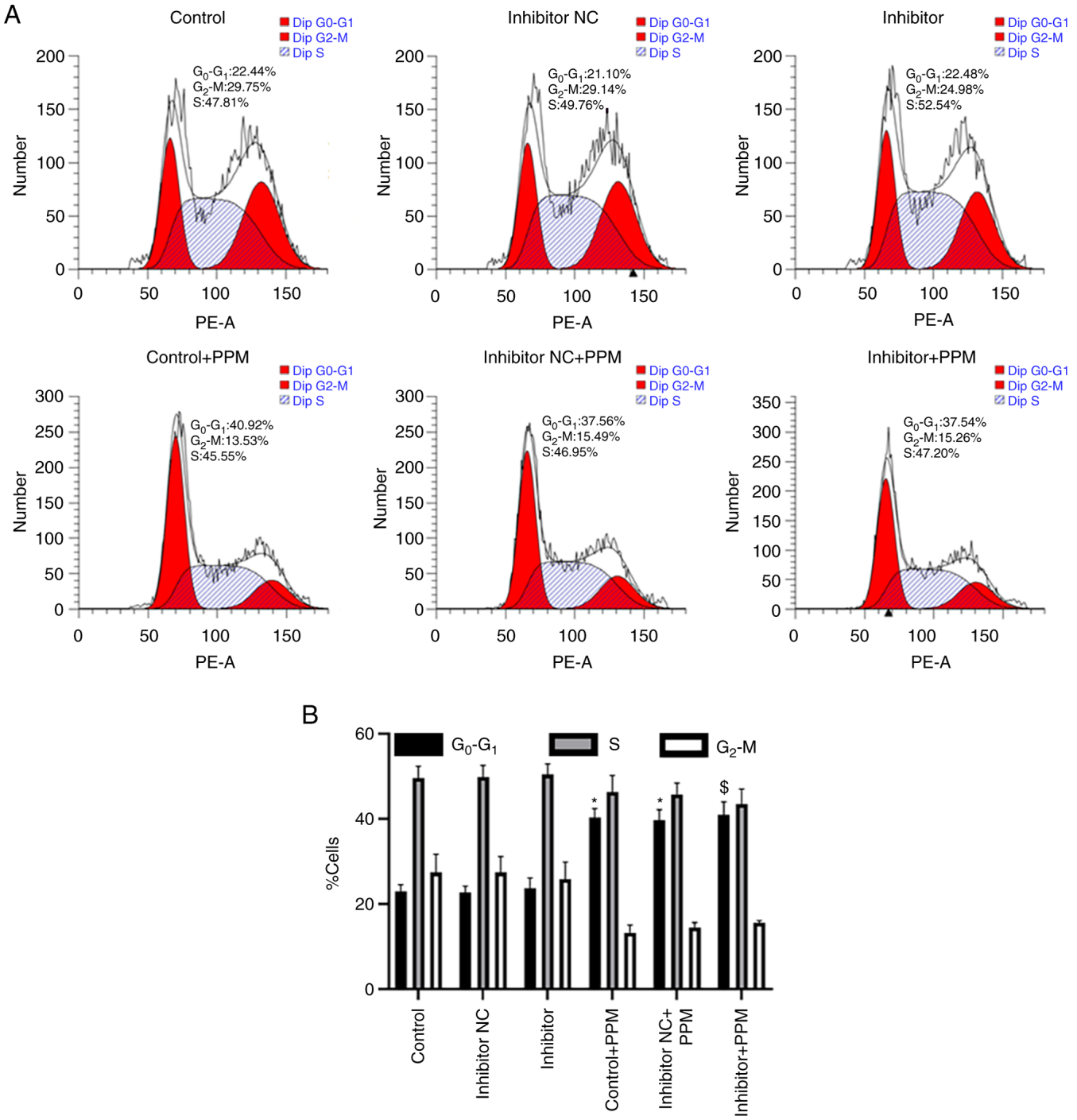

Figure 5. PPM regulates HepG2 cell cycle progression independently of miR-26b-5p. (A) Cell cycle phase distribution was assessed in HepG2 cells, including G_0/G_1, S and G_2/M. (B) Quantitative data of HepG2 cells cycle phase distribution. *P<0.05 vs. Control; $P<0.05 vs. Inhibitor. miR, microRNA; NC, negative control; PPM, 1,4,5,6,7,8-hexahydropyrido[4,3-d]pyrimidine.

proteins Bax and Caspase 3, and increases the sensitivity of liver cancer cells to apoptosis (19,20). NF-κB activation is associated with apoptosis and tumorigenesis (12); miR-26b inhibits NF-κB signaling to promote apoptosis of liver cancer cells (19,20). In the present study, miR-26b-5p inhibitor transfection increased p-p65 expression, whereas PPM decreased this induced expression of p-p65, demonstrating that PPM may upregulate miR-26b-5p to promote cell apoptosis, which is associated with activation of NF-κB/p65 (20).

Dual-luciferase reporter assay, western blotting and bioinformatics were used to verified that miR-26b-5p targeted and downregulated the expression of CDK8. Bcl-2 is an oncogene responsible for promoting liver cancer occurrence and metastasis (24); it also inhibits stemness-related protein c-Myc (25) and reduces breast cancer cell proliferation (26). The present study results indicated that PPM upregulation of miR-26b-5p suppresses NF-κB/p65 signaling pathway in HepG2 cells by targeting of CDK8.The present study verified the association between CDK8 and NF-κB/p65 by OE experiments and western blotting.

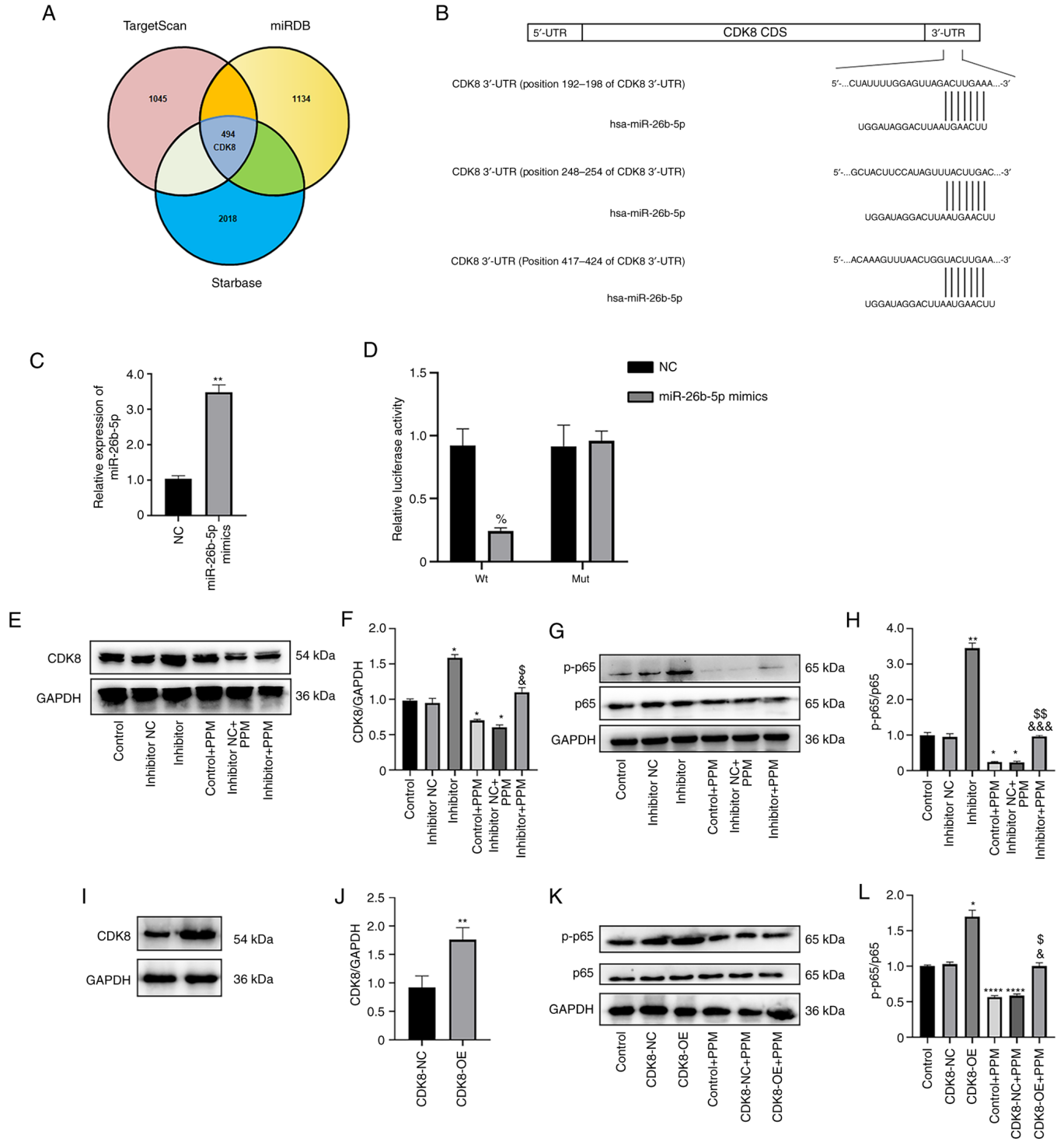

Figure 6. CDK8 is a potential target of miR-26b-5p. (A) Venn diagram of the overlapping predicted target genes of miR-26b-5p from TargetScan, miRDB and Starbase. (B) Three predicted target sites of miR-26b-5p in CDK8 were identified from TargetScan, miRDB and Starbase. (C) Reverse transcription-quantitative PCR showed that miR-26b-5p was upregulated in HepG2 cells after adding miR-26b-5p mimics. **P<0.01 vs. NC mimics. (D) Dual-luciferase reporter assay results demonstrated an interaction between miR-26b-5p and CDK8. $^{\%}$P<0.05 vs. NC. (E) The protein expression levels of CDK8 in the HepG2 cells were detected by western blot. (F) Semi-quantification of the western blot data in (E), from there independent experiments. (G) Western blot analysis was performed to detect the protein expression levels of p65 and p-p65 in HepG2 cells. (H) p-p65 to total p65 ratio of each group. *P<0.05, **P<0.01 vs. Control; $^{\&\&\&}$P<0.001 vs. Control + PPM; $^{\$\$}$P<0.01 vs. Inhibitor. (I) Representative western blots and (J) semi-quantitative expression of CDK8 protein expression levels following transfection of the CDK8-OE vector. **P<0.01 vs. CDK8-NC. (K) Representative western blots and (L) semi-quantitative expression of p65 and p-p65 following CDK8-OE vector transfection and treated with PPM. GAPDH expression was used as a loading control. *P<0.05, ****P<0.0001 vs. Control; $^{\&}$P<0.05 vs. Control + PPM; $^{\$}$P<0.05, vs. Inhibitor. CDS, coding sequence; hsa, *Homo sapiens*; miR, microRNA; mut, mutant; NC, negative control; OE, overexpression; p-, phosphorylated; PGK, phosphoglycerate kinase; PPM, 1,4,5,6,7,8-hexahydropyrido[4,3-d]pyrimidine; UTR, untranslated region; wt, wild-type.

CDK8-OE transfection upregulated the expression of NF-κB/p65. Therefore PPM was hypothesized to induce HepG2 cell apoptosis through upregulation of miR-26b-5p and subsequent targeting of CDK8, which leads to the inhibition of NF-κB activation.

Furthermore, PPM induced HepG2 cell arrest in the G_0/G_1 phase without the involvement of miR-26b-5p. Previous studies have demonstrated that miR-26b-5p mimics affect the cell cycle; for example, CAL27 tongue squamous cell carcinoma cells are arrested at the S/G_2 transition (27) and EC9706 human esophageal cancer cells are arrested in G_1 phase (28). However, miR-26b-5p mimics transfection does not induce apoptosis or cell cycle arrest in mouse spermatocyte-derived GC-2 cells (29). Taken together, the aforementioned results suggested that regulation of the cell cycle by miR-26b-5p may be dependent on cell type; further studies are required to verify this.

In the present study, PPM promoted HepG2 cell apoptosis, decreased cell migration and proliferation and inhibited NF-κB/p65 activation by upregulating miR-26b-5p expression. CDK8 was identified as a target gene of miR-26b-5p. The present study provided novel insights into the anti-tumor effects of PPM. However, the lack of miRNA knockout experiments and PPM + miR mimics transfection experiments are limitation of the present study. *In vivo* studies are required to validate the potential use of miR-26b-5p as a therapeutic target for liver cancer and may further prove that PPM is an effective drug in the treatment of liver cancer. The present study data may provide a basis for further investigation of PPM as a promising drug for the treatment of liver cancer.

Acknowledgements

Not applicable

Funding

The present study was supported by Technology Project of Yantai (grant no. 2022XDRH003).

Availability of data and materials

All data generated or analyzed during this study are included in this published article.

Authors' contributions

HL and YH confirm the authenticity of all the raw data. HL performed the experiments and statistical analysis and wrote the manuscript. YY performed western blotting. YZ performed the cell culture. XB designed the experiments. YH designed the experiments. All authors have read and approved the final manuscript.

Ethics approval and consent to participate

Not applicable.

Patient consent for publication

Not applicable.

Competing interests

The authors declare that they have no competing interests.

References

1. Yang X, Qu S, Wang L, Zhang H, Yang Z, Wang J, Dai B, Tao K, Shang R, Liu Z, *et al*: PTBP3 splicing factor promotes hepatocellular carcinoma by destroying the splicing balance of NEAT1 and pre-miR-612. Oncogene 37: 6399-6413, 2018.
2. Wang Y, Yang L, Chen T, Liu X, Guo Y, Zhu Q, Tong X, Yang W, Xu Q, Huang D and Tu K: A novel lncRNA MCM3AP-AS1 promotes the growth of hepatocellular carcinoma by targeting miR-194-5p/FOXA1 axis. Mol Cancer 18: 28, 2019.
3. Nelson KM, Dahlin JL, Bisson J, Graham J, Pauli GF and Walters MA: The essential medicinal chemistry of curcumin. J Med Chem 60: 1620-1637, 2017.
4. Yin DL, Liang YJ, Zheng TS, Song RP, Wang JB, Sun BS, Pan SH, Qu LD, Liu JR, Jiang HC and Liu LX: EF24 inhibits tumor growth and metastasis via suppressing NF-kappaB dependent pathways in human cholangiocarcinoma. Sci Rep 6: 32167, 2016.
5. Li N, Xin WY, Yao BR, Cong W, Wang CH and Hou GG: N-phenylsulfonyl-3,5-bis(arylidene)-4-piperidone derivatives as activation NF-κB inhibitors in hepatic carcinoma cell lines. Eur J Med Chem 155: 531-544, 2018.
6. Yao BR, Sun Y, Chen SL, Suo HD, Zhang YL, Wei H, Wang CH, Zhao F, Cong W, Xin WY and Hou GG: Dissymmetric pyridyl-substituted 3,5-bis(arylidene)-4-piperidones as anti-hepatoma agents by inhibiting NF-κB pathway activation. Eur J Med Chem 167: 187-199, 2019.
7. Sun Y, Gao ZF, Yan WB, Yao BR, Xin WY, Wang CH, Meng QG and Hou GG: Discovery of novel NF-κB inhibitor based on scaffold hopping: 1,4,5,6,7,8-hexahydropyrido[4,3-d]pyrimidine. Eur J Med Chem 198: 112366, 2020.
8. Zhou YQ, Sun Y, Luo HL, Gao ZF, Zhang HQ, Meng QG, Bai XY, Hou GG and Hou Y: Discovery of anti-hepatoma agents from 1,4,5,6,7,8-hexahydropyrido[4,3-d]pyrimidine by inhibiting PI3K/AKT/NF-κB pathway activation. Eur J Med Chem 225: 113796, 2021.
9. Iacona JR and Lutz CS: miR-146a-5p: Expression, regulation, and functions in cancer. Wiley Interdiscip Rev RNA 10: e1533, 2019.
10. Gao X, Han D and Fan W: Down-regulation of RBP-J mediated by microRNA-133a suppresses dendritic cells and functions as a potential tumor suppressor in osteosarcoma. Exp Cell Res 349: 264-272, 2016.
11. Nussbacher JK and Yeo GW: Systematic discovery of RNA binding proteins that regulate MicroRNA levels. Mol Cell 69: 1005-1016.e7, 2018.
12. Du Q, Yuan Z, Huang X, Huang Y, Zhang J and Li R: miR-26b-5p suppresses chemoresistance in breast cancer by targeting serglycin. Anticancer Drugs 33: 308-319, 2022.
13. Miyamoto K, Seki N, Matsushita R, Yonemori M, Yoshino H, Nakagawa M and Enokida H: Tumour-suppressive miRNA-26a-5p and miR-26b-5p inhibit cell aggressiveness by regulating PLOD2 in bladder cancer. Br J Cancer 115: 354-363, 2016.
14. Lin Y, Jian Z, Jin H, Wei X, Zou X, Guan R and Huang J: Long non-coding RNA DLGAP1-AS1 facilitates tumorigenesis and epithelial-mesenchymal transition in hepatocellular carcinoma via the feedback loop of miR-26a/b-5p/IL-6/JAK2/STAT3 and Wnt/β-catenin pathway. Cell Death Dis 11: 34, 2020.
15. Khosla R, Hemati H, Rastogi A, Ramakrishna G, Sarin SK and Trehanpati N: miR-26b-5p helps in EpCAM+cancer stem cells maintenance via HSC71/HSPA8 and augments malignant features in HCC. Liver Int 39: 1692-1703, 2019.
16. Liu S, Li L, Li M and Zhang J: Effect of miR-26b-5p on cis-diamine dichloroplatinum-induced ovarian granulosa cell injury by targeting MAP3K9. In Vitro Cell Dev Biol Anim 56: 213-221, 2020.
17. Wu T, Chen W, Liu S, Lu H, Wang H, Kong D, Huang X, Kong Q, Ning Y and Lu Z: Huaier suppresses proliferation and induces apoptosis in human pulmonary cancer cells via upregulation of miR-26b-5p. FEBS Lett 588: 2107-2114, 2014.
18. Zhu L and Mei M: Interference of long non-coding RNA HAGLROS inhibits the proliferation and promotes the apoptosis of ovarian cancer cells by targeting miR-26b-5p. Exp Ther Med 22: 879, 2021.
19. Feng Y, Zu LL and Zhang L: MicroRNA-26b inhibits the tumor growth of human liver cancer through the PI3K/Akt and NF-κB/MMP-9/VEGF pathways. Oncol Rep 39: 2288-2296, 2018.

20. Zhao N, Wang R, Zhou L, Zhu Y, Gong J and Zhuang SM: MicroRNA-26b suppresses the NF-κB signaling and enhances the chemosensitivity of hepatocellular carcinoma cells by targeting TAK1 and TAB3. Mol Cancer 13: 35, 2014.
21. Chen Y, Li S, Zhang Y, Wang M, Li X, Liu S, Xu D, Bao Y, Jia P, Wu N, *et al*: The lncRNA Malat1 regulates microvascular function after myocardial infarction in mice via miR-26b-5p/Mfn1 axis-mediated mitochondrial dynamics. Redox Biol 41: 101910, 2021.
22. Zhang R, Niu Z, Pei H and Peng Z: Long noncoding RNA LINC00657 induced by SP1 contributes to the non-small cell lung cancer progression through targeting miR-26b-5p/COMMD8 axis. J Cell Physiol 235: 3340-3349, 2020.
23. Han F, Huang D, Huang X, Wang W, Yang S and Chen S: Exosomal microRNA-26b-5p down-regulates ATF2 to enhance radiosensitivity of lung adenocarcinoma cells. J Cell Mol Med 24: 7730-7742, 2020.
24. Wilke CM, Hess J, Klymenko SV, Chumak VV, Zakhartseva LM, Bakhanova EV, Feuchtinger A, Walch AK, Selmansberger M, Braselmann H, *et al*: Expression of miRNA-26b-5p and its target TRPS1 is associated with radiation exposure in post-Chernobyl breast cancer. Int J Cancer 142: 573-583, 2018.
25. Zhang X, Zhang X, Wang T, Wang L, Tan Z, Wei W, Yan B, Zhao J, Wu K, Yang A, *et al*: MicroRNA-26a is a key regulon that inhibits progression and metastasis of c-Myc/EZH2 double high advanced hepatocellular carcinoma. Cancer Lett 426: 98-108, 2018.
26. Li J, Li X, Kong X, Luo Q, Zhang J and Fang L: MiRNA-26b inhibits cellular proliferation by targeting CDK8 in breast cancer. Int J Clin Exp Med 7: 558-565, 2014.
27. Yi L, Liu Y, Xu A, Li S, Zhang H, Peng M, Li Z, Ren H, Dai J, Luo C, *et al*: MicroRNA-26b-5p suppresses the proliferation of tongue squamous cell carcinoma via targeting proline rich 11 (PRR11). Bioengineered 12: 5830-5838, 2021.
28. Zhang K, Zhang B, Bai Y and Dai L: E2F1 promotes cancer cell sensitivity to cisplatin by regulating the cellular DNA damage response through miR-26b in esophageal squamous cell carcinoma. J Cancer 11: 301-310, 2020.
29. Liu Y, Liu WB, Liu KJ, Ao L, Cao J, Zhong JL and Liu JY: Overexpression of miR-26b-5p regulates the cell cycle by targeting CCND2 in GC-2 cells under exposure to extremely low frequency electromagnetic fields. Cell Cycle 15: 357-367, 2016.